"Water-free" computer model for fluid bilayer membranes

Oded Farago[a)]
Materials Research Laboratory, University of California, Santa Barbara, California 93106

(Received 31 December 2002; accepted 8 April 2003)

We use a simple and efficient computer model to investigate the physical properties of bilayer membranes. The amphiphilic molecules are modeled as short rigid trimers with finite range pair interactions between them. The pair potentials have been designed to mimic the hydrophobic interactions, and to allow the simulation of the membranes without the embedding solvent as if the membrane is in vacuum. We find that upon decreasing the area density of the molecules the membrane undergoes a solid–fluid phase transition, where in the fluid phase the molecules can diffuse within the membrane plane. The surface tension and the bending modulus of the fluid membranes are extracted from the analysis of the spectrum of thermal undulations. At low area densities we observe the formation of pores in the membrane through which molecules can diffuse from one layer to the other. The appearance of the pores is explained using a simple model relating it to the area dependence of the free energy. © *2003 American Institute of Physics.*
[DOI: 10.1063/1.1578612]

I. INTRODUCTION

When amphiphilic molecules such as lipids are brought into contact with water they tend to arrange so as to shield their "oily" hydrocarbon tail from the aqueous environment while exposing their hydrophilic head to the water. One of the simplest structures formed in this way is of a bilayer membrane—a double sheet of surfactants separating two aqueous phases.[1] Bilayer membranes are common in biological systems.[2] Living cells are separated from their extracellular surroundings by plasma membranes that control the transport of material into and out of the cell.[3,4] Most biological membranes are found in the fluid phase where the lipids comprising the bilayer can diffuse freely in the membrane plane. Another characteristic feature of lipid bilayers is their high flexibility which allows for large thermally excited undulations.[5,6] The fluidity and low rigidity of membranes are important for many of their biological properties, such as their ability to change their shape easily and the possibility of proteins to insert themselves into the membrane.[7]

The thickness of membranes is comparable to the size of the constituting surfactant molecules (typically on the nanometer scale), while their lateral extension can greatly exceed their thickness and reach up to several micrometers. Consequently, coarse-grain phenomenological models, such as Ginzburg–Landau free energy functionals[8] or the effective surface Hamiltonian,[5,6,8,9] have been used in order to study the physical properties of membranes, as well as of other interfaces (like surfactants monolayer in microemulsions or vapor–fluid interfaces). In those theories the bilayer membrane is treated as a smooth continuous surface, and its elastic energy is related to the membrane area and the local curvatures. These theories have been very successful in describing the shape and phase diagrams of bilayer membranes.[10,11]

Phenomenological models describe the mesoscopic physical behavior of interfaces and membranes, but do not allow one to approach these systems on the molecular level. Many theories have been developed in an attempt to understand how the mesoscopic behavior emerges from the microscopic entities and the interactions between them. These theories include lattice "Ising-like" models,[8] molecular theories of the hydrocarbon chain packing,[12] theories including the effect of electrostatic interactions,[13] and density functional theories.[14] The most microscopic detailed approach is employed in some computer simulations where the amphiphiles and water, and the interactions between them are modeled explicitly in full detail.[15] Since these simulations require an enormously large computing time, they are restricted to fairly small systems consisting of 50–200 amphiphiles, and can be utilized to investigate phenomena occurring on short time scales of a few nanoseconds. In order to study mesoscale phenomena it is therefore necessary to dispense with some of the microscopic details in the simulations and use simplified models.[16] A number of such simplified computer models have been devised by several groups. In these models the structure of the surfactant molecules is represented in a "coarse-grained" manner where a number of atoms are grouped together into a single site. The first level of coarse graining is obtained by replacing the water molecules and the CH_2 groups of the hydrocarbon chain by unified atoms.[17–19] This can reduce the number of atoms per lipids to about 50. Much more simplified models, in which the amphiphiles consists of only 5–10 atoms, were also presented.[20–22] In these latter models the electrostatic potentials are usually ignored and the potentials of the chemical bonds are greatly simplified. At this level of simplification it is obviously impossible to address specific lipids systems, but rather the more general properties of self-assembling systems.

[a)]Also at: Department of Physics, Korea Advanced Institute of Science and Technology (KAIST), 373-1 Kusong-dong, Yusong-gu, Taejon 305-701, South Korea. Electronic mail: farago@mrl.ucsb.edu

The size of amphiphilic systems which can be simulated using simplified models is constantly growing by virtue of the availability of inexpensive and powerful commodity PC hardware and due to the development of new simulation techniques such as dissipative particle dynamics (DPD).[23] Simulations of model systems consisting of $N \gtrsim 1000$ lipids have been recently reported in the literature.[23–25] The major restriction on the size of the systems in these simulation stems from the large number of atoms included in the simulation cell which is typically an order of magnitude larger than the number of amphiphilic molecules. The low ratio between the number of lipids and the *total* number of atoms is due to two factors. The first one is the number of atoms comprising each lipid molecule which, as discussed above, can vary from 50 to 5 depending on the level of simplification employed in the simulations. The second factor is the number of water molecules in the simulation cell. In bilayers simulations the typical number ratio of water to lipid molecules is in the range from 10 to 30.[15,17–22] A great fraction of the computing time is, thus, "wasted" on the simulations of the water even when the water molecules are represented by a single (unified) atom. Only very few models have so far been proposed in which the amphiphiles are simulated without the presence of water. The major difficulty in establishing such "water-free" models is the need to mimic the hydrophobic effect that prevents the amphiphilic molecules from leaving the aggregate into the solvent. Drouffe *et al.*[26] and Noguchi *et al.*[27] have used *ad hoc* multibody potentials to overcome this problem. With the aid of these nonphysical potentials they have managed to observe the formation of fluid vesicles in their simulations. La Penna *et al.*[28] have studied a water-free flat bilayer model with Lennard-Jones (LJ) potentials that depend on the relative orientation of the lipids (and which are closely related to the Gay–Berne[29] potentials used in liquid crystals simulations). With this model they have been able to simulate bilayer membranes in both the solid and the gel phases. Fluid membranes, however, were found unstable against lipids evaporation from the membrane plane.

In this paper we present an exceptionally simple computer model of a *fluid* bilayer membrane. Our model has the following features: (a) It is a water-free model, i.e., we simulate the membrane without the presence of water. (b) The "lipids" forming the membranes consist of only three atoms, one representing the hydrophilic headgroup and the other two the hydrophobic tail. These three atoms are "glued" to each other to form a rigid linear trimer (the lipid), and have no additional interactions between them. (c) The different lipids interact through finite range (truncated) LJ interactions between their three sites. The parameters of the LJ potentials are fixed and do *not* depend neither on the relative orientation of the lipids (as in Ref. 28), nor on their local density (i.e., there are no multibody interactions in our model). The above-mentioned properties make our membrane model computationally very efficient (albeit a less "flexible" one in comparison to other simplified models with more interaction sites per amphiphile). To investigate the statistical mechanical properties of the membrane, we have performed a set of Monte Carlo (MC) simulations where for each MC run we have fixed the temperature, the number of lipids, and the projected area of the membrane. The projected area serves as the control parameter in our simulations, and we have investigated the phase behavior of the membrane as a function of it. We found that upon increasing the projected area (i.e., reducing the area density of the lipids) the membrane undergoes a solid–fluid phase transition. In the solid phase the lipids are not mobile and they pack in a hexagonal order. In the fluid phase the lipids are free to diffuse in the membrane plane. We have measured the spectrum of thermal undulations of the fluid membranes from which we have extracted the surface tension and the bending modulus that characterize the elastic behavior of the membrane. At low area densities we found another transition from negative to positive surface tension, accompanied by the formation of pores in the membranes. Such a behavior is indeed predicted by theoretical arguments.[30–32]

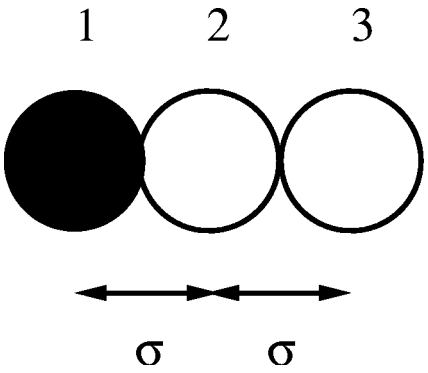

FIG. 1. A schematic picture of a lipid molecule in our model system—a rigid linear trimer consisting of three atoms whose centers are separated a distance σ apart. The atom labeled 1 (solid circle) represents the hydrophilic head of the lipid, while the atoms labeled 2 and 3 (open circles) represent the hydrophobic tail.

The paper is organized as follows: In Sec. II we present our computer model, and discuss the details of the simulations. In Sec. III we describe the physical properties of the systems as obtained by the simulations. Section III is divided into three sections dealing, respectively, with the phase diagram of the system, its spectrum of thermal undulations and elastic properties, and the appearance of holes in membranes with large projected area. We summarize and discuss the results in Sec. IV.

II. DETAILS OF THE MODEL AND THE SIMULATIONS

The lipids in our model system consist of three spherical atoms connected to form a linear trimer. The lipid molecules are rigid—they do not bend and the distance σ between the center of the atoms is *fixed* (see Fig. 1). We set $\sigma = 1$ as our unit length scale throughout this paper. We shall label the three atoms forming each lipid as 1, 2, and 3. Atom 1 represents the hydrophilic head of the lipid, while atoms 2 and 3 represent its hydrophobic tail. The different lipids interact with each other via spherically symmetric pair potentials between their constituting atoms. The pair potential $U_{ij}(r)$ depicts the interactions between atom i and atom j of two different molecules separated a distance r apart. The pair

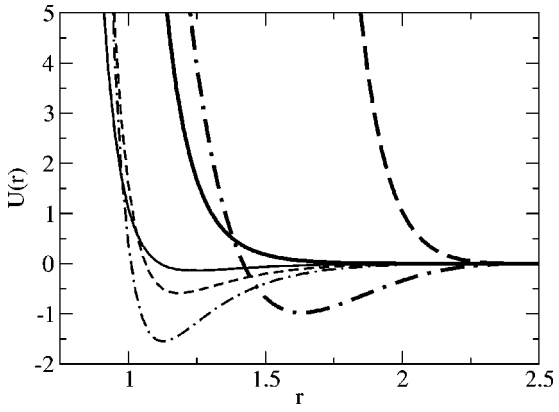

FIG. 2. The different pair potentials $U_{ij}(r)$ used in our model: U_{11} (solid line), U_{22} (dashed line), U_{33} (dotted–dashed line), U_{12} (bold solid line), U_{13} (bold dashed line), and U_{23} (bold dotted–dashed line). The distance r is in units of σ (see definition in text), while the potentials U_{ij} are in kT units. The parameters σ_{ij} and ϵ_{ij} [see Eqs. (1)–(5)] are as follows: $\sigma_{11}=1.1\sigma$, $\sigma_{22}=1.05\sigma$, $\sigma_{33}=\sigma$, $\sigma_{12}=1.15\sigma$, $\sigma_{13}=1.4\sigma$, $\sigma_{23}=0.525\sigma$, $\epsilon_{11}=0.1875kT$, $\epsilon_{22}=1.75kT$, $\epsilon_{33}=1.875kT$, $\epsilon_{12}=1.1375kT$, $\epsilon_{13}=200kT$, and $\epsilon_{23}=375kT$.

potentials U_{12} and U_{13} describe the interaction between hydrophobic and hydrophilic particles. They are given by the purely repulsive LJ potential

$$U_{12}^{\mathrm{LJ}}(r)=4\epsilon_{12}\left(\frac{\sigma_{12}}{r}\right)^{12} \tag{1}$$

and

$$U_{13}^{\mathrm{LJ}}(r)=4\epsilon_{13}\left(\frac{\sigma_{13}}{r}\right)^{18}. \tag{2}$$

The pair potentials U_{11}, U_{22}, and U_{33} describe the interactions between two similar atoms, both either hydrophobic or hydrophilic. They are given by the attractive LJ potentials

$$U_{ii}^{\mathrm{LJ}}(r)=4\epsilon_{ii}\left[\left(\frac{\sigma_{ii}}{r}\right)^{12}-\left(\frac{\sigma_{ii}}{r}\right)^{6}\right], \tag{3}$$

where $i=1, 2, 3$. Finally, the interaction between the hydrophobic particles 2 and 3 is also depicted by an attractive LJ potential, but of the form

$$U_{23}^{\mathrm{LJ}}(r)=4\epsilon_{23}\left[\left(\frac{\sigma_{23}}{r}\right)^{2}-\left(\frac{\sigma_{23}}{r}\right)\right]. \tag{4}$$

All pair potentials are truncated at the same cutoff $r_c=2.5\sigma$, and the discontinuity at r_c is avoided by adding extra terms to the LJ potentials that ensure the vanishing of the potential, as well as of its first and second derivative, at $r=r_c$. The final form of the pair potentials is thus given by

$$U_{ij}(r)=U_{ij}^{\mathrm{LJ}}(r)-U_{ij}^{\mathrm{LJ}}(r_c)-\left.\frac{\partial U_{ij}^{\mathrm{LJ}}(r)}{\partial r}\right|_{r=r_c}(r-r_c)$$

$$-\frac{1}{2}\left.\frac{\partial^2 U_{ij}^{\mathrm{LJ}}(r)}{\partial r^2}\right|_{r=r_c}(r-r_c)^2. \tag{5}$$

The different pair potentials are depicted in Fig. 2. The values of the parameters σ_{ij} (in units of σ) and ϵ_{ij} (in kT units, where T is the temperature and k the Boltzmann constant) used in the simulations are summarized in the caption on Fig. 2.

The pair potentials in our computer model have been designed to allow, on the one hand, the diffusion of molecules in the plane of the membrane but to restrict, on the other hand, their motion in the third direction. We have tested various models before we arrived to the one that we have used in the simulations. The original idea was to use dimers with one hydrophilic and one hydrophobic particles, and to describe the interactions between them by 6-12 LJ potentials [Eq. (3)] and a 12-power repulsive potential [Eq. (1)], depending on whether the atoms are of the same or different species. It turned out that the membranes depicted by such a model were unstable against the extraction of molecules from the membrane plane. To increase the membrane stability we added a third hydrophobic atom to the lipids. The pair interactions between this atom and the other two atoms are described by different forms of LJ potentials: For the interaction with the hydrophilic atom labeled 1 we use the more repulsive 18-power LJ potential U_{13} [Eq. (2)], while for the interaction with the hydrophobic atom labeled 2 we use the 1–2 LJ potential U_{23} [Eq. (4)]. The former potential establishes a strong repulsion between the hydrophobic and the hydrophilic parts of the lipids, thus reducing significantly (eliminating on the time scale of the simulations) the escape probability of molecules (more on this point in the next paragraph). The latter has a very shallow minimum which allows a greater mobility of the lipids in the membrane plane (by making small the energy changes due to a relative motion of the lipids with respect to each other). We have gone through a rather lengthy ''trial and error'' process of fine tuning the parameters σ_{ij} and ϵ_{ij} which control the range of pair repulsion and the depth of the attractive potential wells. Their values have been set to (a) make favorable the alignment of molecules next to each other at a distance slightly larger than σ, and (b) to make the attraction between molecules sufficiently strong to support the stability of the membrane, but not too strong to the extent that would entirely prevent the diffusion of the lipids.

It is not an easy task to form a fluid bilayer sheet in a model system that does not contain water. Membranes become fluid at low area densities and high temperatures, and under these conditions the lipids tend to escape quite easily from the membrane plane. It is the water that confines the lipids to the membrane. In the absence of water molecules this role has to be played by the hydrophobic heads which must form some sort of geometric or dynamic constraint for the extraction of lipids. In our model we establish such a constraint by making the excluded volume part of the pair potentials U_{ij} *nonadditive*, namely we make the size of a particle i ''seen'' by another particle i smaller than its size as seen by a particle j of a different species. We can define the distance a_{ij} at which the pair potential between them $U_{ij}=kT$ as a measure for the range of hard core repulsion between the two particles i and j. (It is unlikely to find a pair i and j separated by a smaller distance.) It is customary to regard a_{ii} as the diameter of atom i and, with this interpretation, to expect for the additivity of the hard core diameters,

i.e., to have $a_{ij} \simeq (a_{ii}+a_{jj})/2$ for $i \neq j$. In our model we do not find this property (see Fig. 2). The pair potentials in our system describe the effective interactions between the different atoms and they include the effect of the water molecules which are not simulated explicitly. Therefore, there is no a priori reason why the effective diameters associated with different particles should be strictly additive. The increased range of hard core repulsion between the hydrophilic atom 1 and the hydrophobic atoms 2 and 3 is designed to compensate for the absence of water from the simulation cell.

The simulations were performed with membranes consisting of $N=1000$ lipids (500 lipids in each layer) with periodic boundary conditions in the membrane (x,y) plane, and with no boundaries in the normal z direction. Subsequent MC configurations were generated by two types of move attempts: translations of lipids and rotations around the mid (second) atom. The MC unit time is defined as the time (measured in number of MC configurations) in which, on the average, we attempt to move and rotate each molecule once. The acceptance probability of both types of moves was approximately half. We performed a set of simulations of membranes with the same temperature T and number of lipids N, and with varying projected areas. For each value of the projected area we studied eight different membranes starting at different initial configurations. The initial configurations were created by randomly placing 500 lipids in two layers with a vertical (along the normal z direction) separation σ between the atoms labeled 3 in the two layers, and with all the lipids oriented normal to the membrane plane. The initial configurations were then "thermalized" over a period of 5×10^5 MC time units, followed by a longer period of 6×10^6 time units during which quantities of interest were evaluated. The duration of the MC runs is substantially larger than the relaxation time which we estimated in various ways: As a first approximation for the relaxation time we used the time it took the potential energy of the membrane to saturate from its high initial value (resulting from overlap of particles in the random initial configuration) to a final "typical" value. This time was of the order of 10^4 MC time units. An independent estimate of the relaxation time was obtained from a study of the spectrum of thermal undulations of the membranes (see more details, later in the text). Inspection of the autocorrelation function of the amplitude of the longest wavelength mode led to a similar estimate of 10^4 time units for the relaxation time. A more conservative estimate can be obtained from measurements of the self-diffusion constant of the lipids in the fluid phase (see, again, later in the text). The relaxation time can be associated with the time it takes a molecule to diffuse a distance equal to the pair potentials cutoff (2.5σ). The relaxation time obtained using this criterion was an order of magnitude larger ($\sim 10^5$ MC time units), still smaller than the equilibration time, and much smaller than the total length of the simulations.

III. SIMULATION RESULTS

A. Phase diagram

The projected area of the membranes in the simulations ranges from $A_p = L_p^2 = (26.875)^2$ to $A_p = (30.625)^2$ with intervals of $\Delta L_p = 0.625$. For all area densities we measured the self-diffusion constant of the molecules relative to the diffusion of the center of mass, defined by

$$D \equiv \lim_{t\to\infty} \frac{\Delta r'(t)^2}{4t} \equiv \lim_{t\to\infty} \frac{1}{4Nt} \sum_{i=1}^{N} [(\vec{r}_i(t) - \vec{r}_{\mathrm{CM}}(t)) - (\vec{r}_i(0) - \vec{r}_{\mathrm{CM}}(0))]^2, \quad (6)$$

where $\vec{r}_i(t)$ denotes the position of the ith lipid (defined by the position of its mid atom) at time t, while $\vec{r}_{\mathrm{CM}}(t)$ denotes the position of the center of mass of lipids.[33] We have also measured the self-diffusion coefficient *in the membrane plane*, defined by

$$D_{x-y} \equiv \lim_{t\to\infty} \frac{1}{4Nt} \sum_{i=1}^{N} \{[(x_i(t) - x_{\mathrm{CM}}(t)) - (x_i(0) - x_{\mathrm{CM}}(0))]^2 + [(y_i(t) - y_{\mathrm{CM}}(t)) - (y_i(0) - y_{\mathrm{CM}}(0))]^2\}, \quad (7)$$

where x and y denote Cartesian coordinates. [In all the simulations the membranes lied in the (x,y) plane, while fluctuating in the normal z direction.] As the lipids can only diffuse within the plane of the membrane, we found no difference between D and D_{x-y}.

At low projected area (high area density) we found the membrane in a solid phase characterized by two features: (a) The diffusion constant of the lipids is vanishingly small.

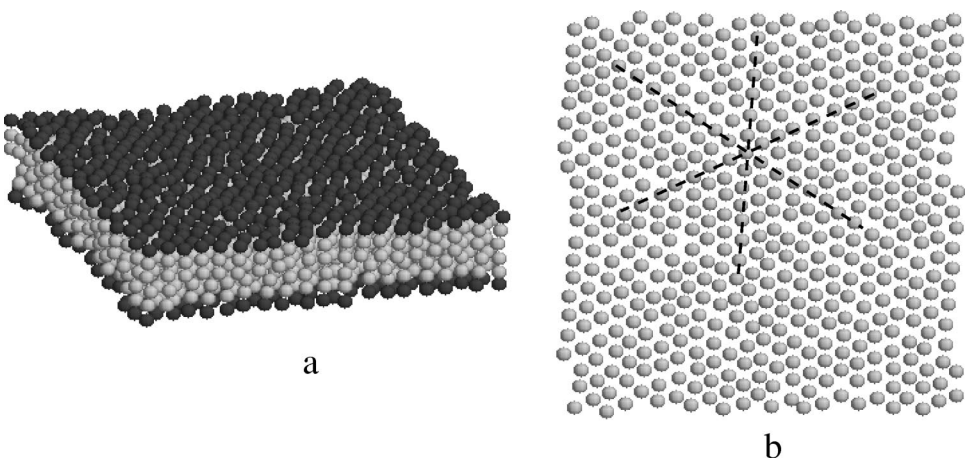

FIG. 3. (a) Equilibrium configuration of a solid membrane with $A_p = (26.875)^2$. The atoms labeled 1 (the "hydrophilic" atoms) are shown as black spheres of diameter σ, while the gray shaded spheres depict the (hydrophobic) atoms labeled 2 and 3, and are of diameter σ as well. (b) A top view of the plane of mid (labeled 2) atoms of the membrane upper layer.

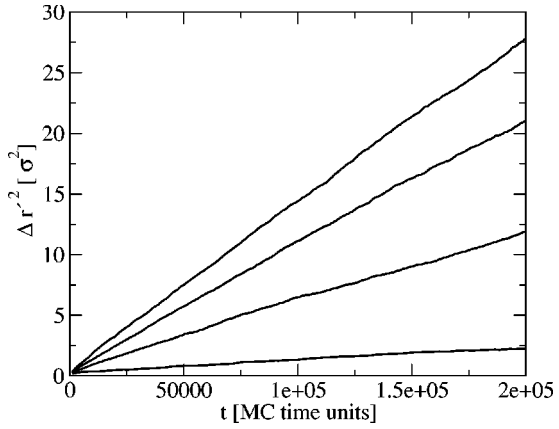

FIG. 4. The lipids mean square displacement $\Delta r'^2$ (measured in σ^2 units) as a function of the time (measured in MC time units) for fluid membranes with (from bottom to top) $A_p=(28.125)^2$, $A_p=(28.75)^2$, $A_p=(29.375)^2$, and $A_p=(30.0)^2$.

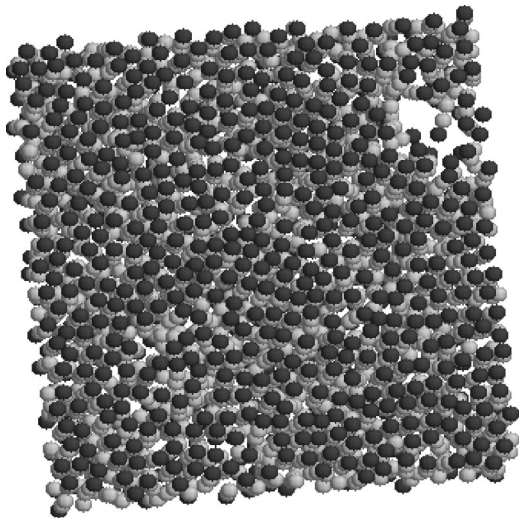

FIG. 6. Equilibrium configuration of a fluid membrane with $A_p=(30.0)^2$ having a pore on its upper right corner.

[The root mean square displacement $\sqrt{\Delta r'^2}$ has barely changed during the course of the simulations, and it has never exceeded the typical distance between neighbor molecules ($\sim\sigma$).] (b) The lipids arrange themselves in a hexagonal order in the membrane plane. A typical equilibrium configuration of a membrane with $A_p=(26.875)^2$ is shown in Fig. 3(a). A top view of the plane of mid (labeled 2) atoms of the membrane upper layer, revealing the hexagonal order of the lipids, is shown in Fig. 3(b). The lattice imperfections observed at Fig. 3(b) should be mainly attributed to the incommensurability of the 500 sites hexagonal lattice with the square simulation cell.

At larger values of the projected area [$A_p \geqslant (28.125)^2$] we found the membranes in a fluid phase. The main feature that distinguishes fluid from solid membranes is the diffusion of the lipids. In Fig. 4 we plot lipids mean square displacement $\Delta r'^2$ [see definition in Eq. (6)] as a function of the simulation time t for fluid membranes with different area densities. The slope of the asymptotically linear curves is four times larger than the self-diffusion constant D. One can observe the growth of D with the increase of the projected area—a rather expected observation as the increase of the projected area means more room for the molecules to move. A typical equilibrium configuration of a fluid membrane with $A_p=(28.75)^2$ is depicted in Fig. 5(a). Another characteristic feature of the fluid membranes is the loss of in-plane hexagonal order, as demonstrated in Fig. 5(b) [compare with Fig. 3(b)].

The membranes with $A_p=(30.0)^2$ exhibited an interesting feature—they developed pores, as demonstrated in the configuration shown in Fig. 6. These pores tended to appear irregularly in the membrane with a characteristic time scale $\tau \gtrsim 2\times 10^5$ for the formation of a pore, and a typical pore lifetime of a few thousand time units. Another interesting phenomenon which we observed for this value of A_p and did not observe at lower projected areas was the occurrence of ''flip–flops''—the transition of lipids from one layer to the other. In Fig. 7 we look at the same membrane depicted in Fig. 6. In this figure, however, we plot only the 500 lipids that were located in the upper layer in the initial configuration. About 30 of them have managed to diffuse from the upper to the lower layer during the course of the simulations. A similar (although not necessarily identical) number of lipids have moved in the opposite direction. *Trans*-bilayer diffusion is an important process in real bilayer membranes.[34] To allow for uniform bilayer growth, some of the lipids must

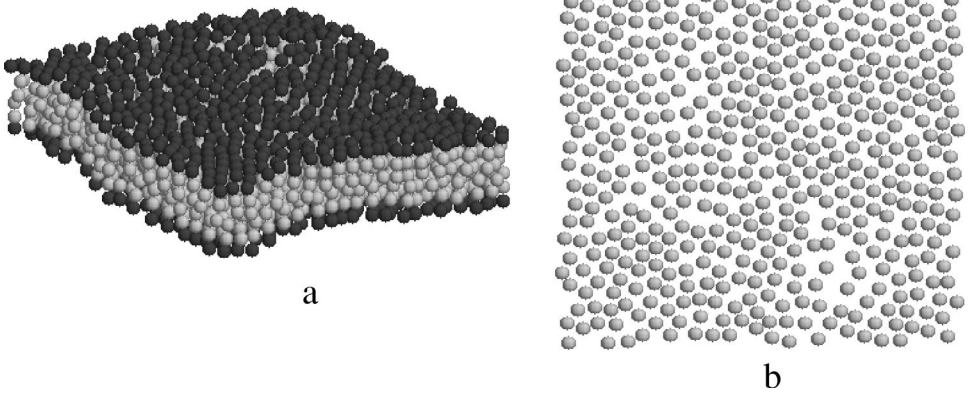

FIG. 5. (a) Equilibrium configuration of a fluid membrane with $A_p=(28.75)^2$. Black and gray atoms (of diameter σ) depict hydrophilic (labeled 1) and hydrophobic (labeled 2 and 3) atoms, respectively. (b) A top view of the plane of mid (labeled 2) atoms of the membrane upper layer.

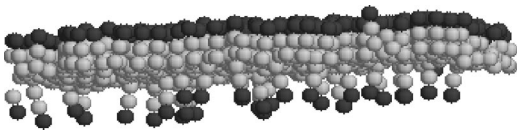

FIG. 7. Another view at the membrane depicted in Fig. 6. Here we show only half of the lipids which were originally located on the upper leaflet of the bilayer.

be transfered from one leaflet to the other during the self-assembly process. When a flat bilayer is bent to form a spherical vesicle, the area of the inner layer becomes smaller than the area of the outer layer, and it is the transition of lipids from the former to the latter that balances their area densities. It has been suggested, based on experiments[35] and computer simulations,[36] that that the formation of pores and the flip–flop motion are closely interconnected. According to these studies, the pores provide a transverse diffusion conduit for the lipids, through which their hydrophilic headgroups cross the hydrophobic region of the membrane. Our study supports the conjecture about the possible relation between pores and flip–flops. In Sec. III C we discuss the origin of the formation of the pores. We show that it is associated with the change in the sign of the membrane surface tension—from a negative to a positive value. Once the surface tension attains a sufficiently large positive value, the energy involved with the formation of the pores is compensated by the reduction in elastic energy.

While the formation of the pores allowed the diffusion of molecules between the two layers, we did not observe [in membranes with $A_p=(30.0)^2$] that pores also lead to the extraction of molecules from the membrane. It is, however, possible that the disassociation of pore-forming membranes occurs on time scales larger than the duration of our simulation. Fast disintegration of the membrane was observed when the projected area was increased to $A_p=(30.625)^2$, which was, therefore, the largest projected area set for the membranes in our study.

B. Elasticity and thermal undulations

On length scales larger than the membrane thickness, the bilayer can be modeled as a smooth continuous sheet. The thermal undulations of the bilayer can be studied with Helfrich Hamiltonian[9] relating the elastic energy to the shape of the membrane,

$$\mathcal{H}=\int_S dA\left[\gamma+\frac{1}{2}\kappa(c_1+c_2-2c_0)^2+\kappa_G c_1 c_2\right]. \tag{8}$$

The integration in the above equation is carried over the whole surface of the membrane. Three elastic moduli are involved with the Helfrich Hamiltonian: the surface tension γ, the bending modulus κ, and the saddle-splay modulus κ_G. The quantities c_1 and c_2 appearing in the above equation are the local principle curvatures of the surface (see a rigorous definition in Ref. 37) which are surface invariants with respect to similarity transformations (translations and rotations), while c_0 is the spontaneous curvature of the surface. For flat bilayers $c_0=0$. It is customary to dispense with the use of the local curvatures in favor of two other (local) invariants: the mean curvature $H\equiv(c_1+c_2)/2$, and the Gaussian curvature $K\equiv c_1c_2$. If one only considers fluctuations which do not change the topology of the membrane, then the total energy associated with the last term in Eq. (8) is a constant.[9] We, thus, arrive to the following more simplified form of Eq. (8):

$$\mathcal{H}=\int_S dA(\gamma+2\kappa H^2). \tag{9}$$

There are various ways to parametrize the surface. One of them is the Monge representation, where the surface is represented by a height function, $z=h(x,y)$, above a reference $x-y$ plane. For a nearly flat surface, i.e., when the derivatives of the height function with respect to x and y are small—$h_x, h_y \ll 1$, one obtains the following approximation for Eq. (9):

$$\mathcal{H}=\int dx\,dy\left[\frac{1}{2}\gamma(h_x^2+h_y^2)+\frac{1}{2}\kappa(\nabla^2 h)^2\right]. \tag{10}$$

Note that unlike Eq. (9), the integral in Eq. (10) runs over the reference (x,y) surface rather than over the actual surface of the membrane.

Equations (8)–(10) are expected to be valid only on length scales larger than the thickness of the membrane. The undulatory motion on smaller length scales (which we did not investigate in this study) is dominated by the so-called "protrusion modes."[38] In our simulations the profile of the bilayers was defined by mapping the system with linear size (of the projected area) L onto an 8×8 grid whose mesh size $l=L/8$ is indeed larger than the typical width of the membrane. The local height of the bilayer was then defined as the average of the local heights of the two layers. The latter were evaluated by the mean height of the lipids (whose positions were identified with the coordinates of their mid atoms) belonging to each layer, which were instantaneously located inside the local grid cell. The discretized form of Hamiltonian (10) is

$$\mathcal{H}=a_0\sum_{\vec{r}}\left[\frac{1}{2}\gamma(h_x^2+h_y^2)+\frac{1}{2}\kappa(\nabla^2 h)^2\right], \tag{11}$$

where the summation goes over the discrete grid coordinates, and $a_0=l^2$ is the area of the grid cells. In Fourier coordinates we define

$$h(\vec{r})=\frac{l}{L}\sum_{\vec{q}} h_{\vec{q}}e^{i\vec{q}\cdot\vec{r}} \tag{12}$$

and

$$h_{\vec{q}}=\frac{l}{L}\sum_{\vec{r}} h(\vec{r})e^{-i\vec{q}\cdot\vec{r}}, \tag{13}$$

where the two-dimensional wave vector $\vec{q}$ has $8^2=64$ discrete values satisfying $\{q_x, q_y=2\pi n/L,\ n=-4, -3,\ldots,2,3\}$. In Fourier space the different modes decouple,

$$\mathcal{H}=\frac{a_0}{2}\sum_{\vec{q}}\left[\gamma|\vec{q}|^2+\kappa|\vec{q}|^4\right]|h_{\vec{q}}|^2, \tag{14}$$

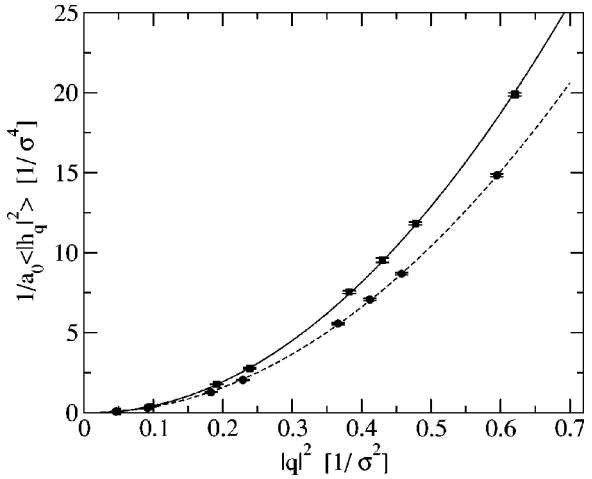

FIG. 8. The inverse of the spectral intensity for undulatory modes $1/a_0\langle|h_q|^2\rangle$ as a function of the square wave number q^2 for membranes with $A_p=(28.75)^2$ (squares) and $A_p=(29.375)^2$ (circles).

and, by invoking the equipartition theorem, we find that the mean square amplitude of the mode $\vec{q}$ (the ''spectral intensity''),

$$a_0\langle|h_{\vec{q}}|^2\rangle=\frac{kT}{(\gamma|\vec{q}|^2+\kappa|\vec{q}|^4)}. \tag{15}$$

The instantaneous amplitudes of the different $\vec{q}$ modes were evaluated using Eq. (13) once in every 100 MC time units, and were averaged over the course of the simulations. To extract the values of γ and κ we used the inverse form of Eq. (15),

$$\frac{1}{a_0\langle|h_{\vec{q}}|^2\rangle}=\frac{(\gamma|\vec{q}|^2+\kappa|\vec{q}|^4)}{kT}, \tag{16}$$

and plotted $1/a_0\langle|h_{\vec{q}}|^2\rangle$ and a function of $|\vec{q}|^2$. The results of the spectral analysis of the undulations for fluid membranes with $(A_p=28.75)^2$ (squares) and $A_p=(29.375)^2$ (circles) are presented in Fig. 8. The error bars represent one standard deviation in the estimates of the averages. The curves depict the best fit of the numerical data to Eq. (16), obtained when γ and κ take the following values:

$$\gamma=-1.4\pm0.2\frac{kT}{\sigma^2},$$
$$\kappa=54\pm2kT, \tag{17}$$

for $A_p=(28.75)^2$, and

$$\gamma=-0.6\pm0.2\frac{kT}{\sigma^2},$$
$$\kappa=42\pm2kT, \tag{18}$$

for $A_p=(29.375)^2$. We verified the validity of Eq. (16) by attempting to fit our data to other polynomial functional forms, including a constants and a $|\vec{q}|^6$ terms. The contributions of these terms to the fit were small, and did not result a significant change in our estimates of γ and κ, based on Eq. (16).

The above values of the bending modulus κ are somewhat larger than the values commonly reported in experiments in phospholipids: $\kappa\sim10-20kT$.[10] We should, in principle, correct our values of κ by considering the reduction in the effectively measured bending modulus due to long-wavelength thermal undulations. The correction term depends logarithmically on the size of the system:[5,39]

$$\frac{\Delta\kappa}{\kappa}=\frac{3kT}{4\pi\kappa}\ln\left(\frac{L}{a}\right), \tag{19}$$

where a is some microscopic length. Setting $a\sim l=L/8$ (the mesh size in our simulations), and using the values of κ in Eqs. (17) and (18), we find that this correction amounts to about 1% of the value of κ and, therefore, falls within the uncertainty in our estimates of the bending modulus.

The fact that the surface tension γ is negative has an interesting implication: It means that the size of the membrane cannot grow indefinitely, but an upper bound exists,

$$L_c\leqslant2\pi\sqrt{\frac{\kappa}{|\gamma|}}, \tag{20}$$

above which there are small q modes with $|\vec{q}|<q_c=2\pi/L_c$ that make the system unstable [see Eq. (14)]. One can also understand the origin of this instability in ''real'' space, rather in q space: When $\gamma<0$ the elastic energy of the membrane *decreases* by increasing its area, and it is the bending energy that stabilizes the system. Modes with larger wavelength (smaller $|\vec{q}|$) require smaller curvatures to increase the area of the membrane and, thus, cost less bending energy. Membranes with linear size $L>L_c$ have long wavelength modes that reduce the elastic area energy more than they increase the bending energy. For systems whose linear size is smaller than, but close to, L_c the amplitude of the small q modes become large [see Eq. (15)], and the approximation in Eqs. (11) and (14) is no longer valid. It is then necessary to include higher order terms in the Hamiltonian (14), and to consider their influence on the spectrum of thermal undulations and on the stability of the membrane.

C. Pore formation

The projected area $\tilde{A}_p$ at which the surface tension vanishes is called the saturated (*Schulman*) area.[40,41] One can evaluate the saturated area of our model membranes using a linear approximation for the relation between the surface tension and the excess area $\delta A_p=A_p-\tilde{A}_p$,[42]

$$\gamma=K_A\left(\frac{\delta A_p}{\tilde{A}_p}\right). \tag{21}$$

The coefficient K_A appearing in the above equations is the area compressibility modulus of the membrane. Using the values of γ obtained from the simulations for $A_p=(28.75)^2\simeq826.6$, and $A_p=(29.375)^2\simeq862.9$ [Eqs. (17) and (18)] in Eq. (21), we derive the following estimates:

$$K_A=19.6\pm6.6\frac{kT}{\sigma^2} \tag{22}$$

and

$$\tilde{A}_p=890\pm17, \tag{23}$$

for K_A and $\tilde{A}_p$. Equation (23) suggests that our membrane with $A_p=(30.0)^2=900$ might be found above the saturated

area $\tilde{A}_p$ and, therefore, may have a positive surface tension. The attempt to verify this conjecture by analyzing the spectrum of the membranes, as done for the fluid membranes with lower projected areas, is hampered by two technical difficulties. The first one is related to the flip–flop motion of lipids between the two leaflets. The *trans*-bilayer diffusion makes it computationally complicated to determine which lipids are related to which layer of the membrane and, therefore, it becomes difficult to calculate the profile of the layers. The other difficulty results from the holes which are created in the membrane. These pores may have an area larger than a_0, the area of the grid cells. In such a case we find an empty cell with no lipids inside, and the height of the membrane at the corresponding grid point cannot be evaluated (unless one interpolates this value using the height of the membrane at the adjacent grid points). We have taken advantage of the fact that the typical time for the appearance of the pores and for the flip–flop motion which accompanies their formation, is larger than the relaxation time of the spectrum, and used short MC runs (during which pores were not observed) to estimate the surface tension of the membrane. We found a positive surface tension with a magnitude of the order of $\gamma \sim 1kT/\sigma^2$, which is roughly half an order of magnitude larger than the value anticipated by Eqs. (21)–(23). While the spectral analysis supports our conjecture that γ is positive for $A_p=(30.0)^2$, one should not attempt to use many independent short runs to achieve a more accurate estimate of γ. It is unclear how well equilibrated the membranes in these short MC runs are. Moreover, it is incorrect to base such an estimate on statistical averaging restricted to membranes without pores. The creation of the pores tends to reduce the surface tension since they make the effective area of the membrane smaller.

Membranes with a positive surface tension can reduce their elastic energy by decreasing their area, and the formation of pores is obviously one of the mechanisms to achieve that. Other ways of reducing the membrane area which are not possible in our model is to decrease the projected area or to increase the area density by adsorbing lipids from the solvent. For the case of a pore formation, one has to consider the line tension energy price involved with the creation of the hole. The simplest theoretical model discussing pore formation was suggested by Litster.[30] In this zero-temperature model, the contribution of a circular hole of radius R_{pore} to the free energy of a membrane with a positive surface tension γ is given by

$$F_{\text{pore}} = -\gamma\pi R_{\text{pore}}^2 + \lambda 2\pi R_{\text{pore}}, \tag{24}$$

where λ is the line tension of the hole. According to this model a pore with a radius larger than the critical value of λ/γ is predicted to grow without bound. Such a thermodynamically large circular hole can be created only if the critical energy barrier $\pi\lambda^2/\gamma$ is accessible by thermal fluctuations. At a finite temperature it is necessary to take into account the entropy of the pores and the picture becomes more complicated. Recent computer simulations[43] have demonstrated that the typical shape of thermally induced pores is noncircular but rather of a self-avoiding ring or a branched polymer. The most striking feature predicted by this study was, however, the fact that pores can appear at zero, and even at small negative surface tension.

The major drawback of the above model is the fact that while it predicts the expansion of the pore without limit, the first term in Eq. (24), assuming a linear relation between the reduction in elastic energy and the area of the pore, applies to small pores only. An improved model can be obtained by assuming other forms of the free energy dependence on the pore area. We first consider a zero temperature model where the membrane does not fluctuate in the normal direction. The free energy of the membrane (which at zero temperature coincides with the potential energy) has a minimum at the saturated area which we shall now denote by $\tilde{A}^E$ [compare this notation with the one used in Eq. (21)] to indicate that it is determined by energy consideration. The subscript p has been omitted since the projected area is also the total area of the membrane in this case. Close to $\tilde{A}^E$ we can use the quadratic approximation to describe the dependence of the free energy density f on the excess area $\delta A^E = A - \tilde{A}^E$,

$$f \equiv \frac{F}{\tilde{A}^E} = \frac{1}{2} K_A^E \left(\frac{\delta A^E}{\tilde{A}^E} \right)^2, \tag{25}$$

where, as in the case of the saturated area, we use the superscript E in the notation of the area compressibility K_A^E. If a pore of area A_{pore} is formed then the area of the membrane is reduced by A_{pore} and, consequently, the pore contribution to the free energy density is given by

$$f_{\text{pore}}(A, A_{\text{pore}}) = \frac{1}{2} K_A^E \left(\frac{\delta A^E - A_{\text{pore}}}{\tilde{A}^E} \right)^2 - \frac{1}{2} K_A^E \left(\frac{\delta A^E}{\tilde{A}^E} \right)^2 + \frac{2\lambda\sqrt{\pi}}{\tilde{A}^E} \sqrt{A_{\text{pore}}}. \tag{26}$$

As in Eq. (24), we consider a circular hole and, thus, its perimeter and area are related by $\Gamma = \sqrt{4\pi A}$. The equilibrium size of the pore A_{pore}^* is found by solving the equation $\partial f_{\text{pore}}/\partial A_{\text{pore}} = 0$, and in addition by verifying that $f_{\text{pore}}(A, A_{\text{pore}}^*) < f_{\text{pore}}(A, 0) = 0$. While in Litster's model a membrane with positive surface tension can be only metastable against the formation of a pore, the model presented here yields a different scenario: Pores are thermodynamically unfavorable as long as the line tension satisfies

$$\lambda > \lambda' = \sqrt{\frac{2}{27\pi}} \frac{(\delta A^E)^{3/2}}{\tilde{A}^E} K_A^E. \tag{27}$$

At this value a first order first transition occurs, and a pore of size $A_{\text{pore}}^* = 2/3\,\delta A^E$ is created. The pore grows gradually as λ is decreased below this value. When $\lambda \to 0$, $A_{\text{pore}}^* \to \delta A^E$, and the effective area of membrane attains the optimal (Schulman) value $\tilde{A}^E$. As in Litster's model, there exists a free energy barrier for the formation of the pore. At the transition ($\lambda = \lambda'$) the height of the barrier is

$$\Delta F \sim \lambda^{4/3} (\delta A^E)^{1/3} / K_A^{E\,1/3}. \tag{28}$$

A theory for the entropic contribution to the free energy of the pore has been recently presented by Sens and Safran.[44]

According to this theory, hole formation is one of the mechanisms to ''redeem'' the degrees of freedom associated with the long wavelength modes in the fluctuation spectrum which are eliminated by the surface tension. To a first approximation, the effect of this entropic surface tension can be easily incorporated into Eqs. (25) and (26). Let us assume for a moment that $K_A^E=0$, and that the projected area of the membrane A_p is fixed. Because of the thermal fluctuations, the total area of the membrane will be larger than A_p. As has been explained in Ref. 44, there exists an optimal total area at which the membrane is tensionless

$$\tilde{A}^S \simeq A_p\left[1+\frac{kT}{8\pi\kappa}\ln\left(\frac{A_p}{l^2}\right)\right], \tag{29}$$

where κ is the bending modulus, and l is some molecular cutoff length. The superscript S denotes the fact that the optimal area discussed here is entropic in nature, and does not need to be equal to $\tilde{A}^E$ in Eq. (25). A membrane with $A\neq\tilde{A}^S$ will experience a surface tension. The free energy associated with this entropic surface tension can be calculated analytically. Here, however, we shall use the quadratic approximation in $\delta A^S\equiv A-\tilde{A}^S$,

$$f\equiv\frac{F}{A_p}=\frac{1}{2}K_A^S\left(\frac{\delta A^S}{A_p}\right)^2, \tag{30}$$

which is valid only close to the minimum of the free energy at $\tilde{A}^S$. The entropic area compressibility in Eq. (30) is given by[44]

$$K_A^S=\frac{32\pi^3\kappa^2}{A_pkT}. \tag{31}$$

Combining the energetic (25) and the entropic (30) contributions to the free energy, we find another quadratic form for the *total* free energy of the membrane

$$f(A)\equiv\frac{F}{A_p}=\frac{1}{2}K_A\left(\frac{\delta A}{A_p}\right)^2, \tag{32}$$

where the excess area $\delta A=A-\tilde{A}$ is defined with respect to the minimum at

$$\tilde{A}=\frac{K_A^EA_p+K_A^S\tilde{A}^S}{\frac{A_p}{\tilde{A}^E}K_A^E+K_A^S}, \tag{33}$$

and the effective area compressibility is equal to

$$K_A=K_A^E\frac{A_p}{\tilde{A}^E}+K_A^S. \tag{34}$$

The optimal area and the area compressibility appearing in the above two equations (and which include both energetic and entropic contributions) should replace their purely energetic counterparts in Eq. (26) for the pore free energy density and in Eqs. (27) and (28) for the critical line tension and the free energy barrier. For typical values of phospholipids: $\kappa=10kT\sim5\times10^{-13}$ ergs, and $A_p=(10\ \mu\text{m})^2=10^{-6}$ cm^2, we get upon substitution in Eq. (31), $K_A^S\sim5\times10^{-3}$ ergs/cm^2. This value of K_A^S is several orders of magnitude smaller than the area compressibility typically found in stretching experiments $K_A\gtrsim10^2$ ergs/cm^2 (Ref. 10) and, therefore, the entropic contribution to K_A and $\tilde{A}$ can be neglected.[45] The effect of the thermal fluctuations can be felt only in small membranes (such as in this paper), as K_A^S increases by decreasing the projected area. Unfortunately, the membranes in our computer study are *too small* to allow the description of this effect by Eqs. (29)–(31). The derivation of these equations is based on the assumption that the long wavelength behavior of the membrane is dominated by the surface tension. This requires that $\kappa(2\pi/\sqrt{A_p})^2\ll\gamma$—a criterion which is not satisfied in our case. The long wavelength fluctuations in our membranes are mainly controlled by the curvature elasticity.

Is the appearance of pores in the simulations in accord with the model described by Eq. (26)? In order to answer this question we need to evaluate the line tension λ of the pore. The line tension λ has the dimensions of energy per unit length. Its magnitude can be estimated by noting that the lipids on the rim of the pore have 1–2 less neighbors compared to the other lipids. Therefore, the energy cost associated with each such lipid is of the order of the interaction energy between two adjacent molecules which is roughly kT. The length occupied by each lipid along the perimeter of the hole is of the order of σ, and so $\lambda\sim kT/\sigma$. This value of λ should be smaller than the critical value λ' given by Eq. (27). Using the values of K_A and $\tilde{A}$ provided by Eqs. (22) and (23), we arrive at the estimate $\lambda'\sim kT/\sigma$ for the membrane with $A_p=30^2=900$ ($\delta A\sim10$). This means that λ and λ' are of the same order of magnitude and, thus, may obey the criterion given by Eq. (27) for the thermodynamic stability of membranes with holes. The fact the pores in our simulations appear for only short time intervals, before they close up, may indicate that λ is, in fact, slightly larger than λ', and that the pores are only metastable. In addition to to the values of λ and λ', we also need to check the free energy barrier for the formation of the pores, as given by Eq. (28). We find $\Delta F\sim kT$, and so the opening of a pore can be nucleated by thermal fluctuations.

IV. SUMMARY AND DISCUSSION

We have introduced a new simple computer model for bilayer membranes whose main feature is the fact that the system is simulated in vacuum rather than in aqueous environment. The elimination of the solvent from the simulations greatly improves computational efficiency. Devising a ''water-free'' model is a great challenge as the water molecules, via the electrostatic interactions between them and the lipids, play a central role in the aggregation and the stabilization of the membrane through the resulting hydrophobic effects. The self-assembly of the system has not been investigated in this paper. (The reader is referred to the simulations presented in Refs. 26 and 27 in which this issue has been addressed.) We did, however, demonstrated that bilayers, once they are formed, can be stable without the surrounding solvent. One only needs to modify the interactions between the lipids, and use effective potentials that compensate for the absence of water by producing a barrier against the disintegration of the membrane. In this model we have

been able to stabilize the membrane using pair-wise short range interactions only—another feature that reduces the computational effort involved with the simulations. To the best of our knowledge, this is the first water-free computer model in which fluid membranes are being observed without the need of multibody interactions.

We have found that our simple model reproduces many known features of bilayer membranes, such as the transition from a high density solid phase to a low density fluid phase. We have inspected the spectrum of thermal fluctuations of the fluid membranes, and found it to be well described by the Helfrich Hamiltonian. From the analysis of the spectral intensity of the different modes, we have extracted the surface tension and bending modulus of the system. Based on our numerical results for the surface tension, we have attempted to determine the optimal area of the membrane at which the surface tension vanishes. Indeed, for areas larger than the saturated area, we have found evidences that the surface tension becomes positive. Fluid membranes with positive surface tension can develop pores, and the creation of pores allows the diffusion of lipids from one layer to the other (flip–flops). The opening of holes in our membranes is in agreement with a simple model that takes into account the contributions to the area compressibility of both the interparticle forces and the thermal fluctuations.

In order to make a closer contact with biological systems, it is necessary to extend the model presented here to include the other elements found in biomemebranes such as the membranes proteins and the cytoskeleton. It would be interesting to see whether these additional components can also be modeled in a coarse-grain manner that would minimize both the computational and the conceptual complexity. Such a model may shed light on an abundance of challenging problems like the effect of the cytoskeleton on the elastic properties of the bilayer, or the role played by the membrane proteins in transport processes across the membrane.

ACKNOWLEDGMENTS

We thank David Andelman, Grace Brannigan, Daan Frenkel, and Thomas Powers for useful discussions, and to Niels Grønbech Jensen and Kurt Kremer for their comments on the paper. Special thanks to Philip Pincus and Claus Jeppesen for their substantial contribution to the work, and to Jeffrey Barteet for technical support. This work was supported by the National Science Foundation under Award No. DMR-0203755. The Materials Research Laboratory at UC Santa Barbara is supported by NSF No. DMR-0080034.

[1] J. Israelachvili, *Intermolecular and Surface Forces* (Academic, London, 1985).
[2] B. Alberts, D. Bray, J. Lewis, M. Raff, K. Roberts, and J. D. Watson, *Molecular Biology of the Cell* (Garland, New York, 1989).
[3] E. Sackmann, H. P. Duwe, and H. Engelhardt, Faraday Discuss. Chem. Soc. **81**, 7136 (1986).
[4] M. Bloom, E. Evans, and O. G. Mouritsen, Q. Rev. Biophys. **24**, 293 (1991).
[5] S. A. Safran, *Statistical Thermodynamics of Surfaces, Interfaces, and Membranes* (Addison-Wesley, New York, 1994).
[6] *Structure and Dynamics of Membranes*, edited by R. Lipowsky and E. Sackmann (Elsevier, Amsterdam, 1995).
[7] R. B. Gennis, *Biomembranes: Molecular Structure and Function* (Springer, New York, 1989).
[8] G. Gompper and M. Schick, "Self-assembling amphiphilic systems," in *Phase Transitions and Critical Phenomena*, edited by C. Domb and J. L. Lebowitz (Academic, London, 1994), Vol. 16.
[9] W. Helfrich, Z. Naturforsch. **28C**, 693 (1973).
[10] U. Seifert and R. Lipowsky, in Ref. 6.
[11] M. Wortis, M. Jarić, and U. Seifert, J. Mol. Liq. **71**, 195 (1997).
[12] I. Szleifer, D. Kramer, A. Ben-Shaul, W. M. Gelbart, and S. A. Safran, J. Chem. Phys. **92**, 6800 (1990).
[13] D. Andelman, in Ref. 6.
[14] E. Chacón, A. M. Somoza, and P. Tarazona, J. Chem. Phys. **109**, 2371 (1998).
[15] H. E. Alper, D. Bassolino, and T. R. Stouch, J. Chem. Phys. **98**, 9798 (1993); K. T. Douglas, J. Tobias, and M. L. Klein, Biophys. J. **69**, 2558 (1995); T. Husslein, D. M. Newns, P. C. Pattnaik, Q. Zhong, P. B. Moore, and M. L. Klein, J. Chem. Phys. **109**, 2826 (1998); I. Z. Zubrzycki, Y. Xu, M. Madrid, and P. Tang, *ibid.* **112**, 3437 (2000).
[16] See review article, J. C. Shelley and M. Y. Shelley, Curr. Opin. Colloid Interface Sci. **5**, 101 (2000).
[17] H. Heller, M. Schaefer, and K. Schulten, J. Phys. Chem. **97**, 8343 (1993).
[18] E. Lindahl and O. Edholn, J. Chem. Phys. **113**, 3882 (2000); Biophys. J. **79**, 426 (2000).
[19] S. J. Marrink and A. E. Mark, J. Phys. Chem. B **105**, 6122 (2001).
[20] B. Smit, P. A. J. Hilbers, K. Esselink, L. A. M. Rupert, N. M. van Os, and A. G. Schlijper, J. Phys. Chem. **95**, 6361 (1991).
[21] R. Goetz and R. Lipowsky, J. Chem. Phys. **108**, 7397 (1998); R. Goetz, G. Gompper, and R. Lipowsky, Phys. Rev. Lett. **82**, 221 (1999).
[22] J. C. Shelley, M. Y. Shelley, R. C. Reeder, S. Bandyopadhyay, and M. L. Klein, J. Phys. Chem. B **105**, 4464 (2001).
[23] D. R. Groot and K. L. Rabone, Biophys. J. **81**, 725 (2001); S. Yamamoto, Y. Maruyama, and S-a. Hyodo, J. Chem. Phys. **116**, 5842 (2002); J. C. Shillcock and R. Lipowsky, *ibid.* **117**, 5048 (2002).
[24] C. F. Lopez, P. B. Moore, J. C. Shelley, M. Y. Shelley, and M. L. Klein, Comput. Phys. Commun. **147**, 1 (2002).
[25] M. Müller, K. Katsov, and M. Schick, J. Chem. Phys. **116**, 2342 (2002).
[26] J. M. Drouffe, A. C. Maggs, and S. Leibler, Science **254**, 1353 (1991).
[27] H. Noguchi and M. Takasu, Phys. Rev. E **64**, 041913 (2001); H. Noguuchi, J. Chem. Phys. **117**, 8130 (2002).
[28] G. La Penna, S. Letardi, V. Minicozzi, S. Morante, G. C. Rossi, and G. Salina, Eur. Phys. J. E **5**, 259 (2001).
[29] J. G. Gay and B. J. Berne, J. Chem. Phys. **74**, 3316 (1981).
[30] J. D. Litster, Phys. Lett. A **53**, 193 (1975).
[31] R. Netz and M. Schick, Phys. Rev. E **53**, 3875 (1996).
[32] M. Müller and M. Schick, J. Chem. Phys. **105**, 8282 (1996).
[33] Note that we use the definition of the diffusion constant in two-dimensional systems $[D \equiv \Delta r'(t)^2/4t]$, rather than it's three-dimensional counterpart $[D \equiv \Delta r'(t)^2/6t]$. The reason for this choice of a definition is the lack of diffusion in the direction normal to the membrane plane.
[34] E. Sackmann, in Ref. 6.
[35] K. Matsuzaki, Biochem. Soc. Trans. **29**, 598 (2001), and references therein.
[36] M. Okazaki, T. Watanabe, N. Urakami, and T. Yamamoto, cond-mat/0204546.
[37] F. David, in *Statistical Mechanics of Membranes and Surfaces*, Proceedings of the Fifth Jerusalem Winter School for Theoretical Physics, edited by D. R. Nelson, T. Piran, and S. Weinberg (World Scientific, Singapore, 1989).
[38] R. Lipowsky and S. Grotehans, Europhys. Lett. **23**, 599 (1993).
[39] L. Peliti and S. Leibler, Phys. Rev. Lett. **54**, 1690 (1985).
[40] J. H. Schulman and J. B. Montagne, Ann. N.Y. Acad. Sci. **92**, 366 (1961).
[41] P. G. de Gennes and C. Taupin, J. Phys. Chem. **86**, 2294 (1982).
[42] The surface tension is the intensive thermodynamic variable conjugate to the projected area, rather than to the total area of the membrane. See discussion in F. David and S. Leibler, J. Phys. II **1**, 959 (1991).
[43] J. C. Schillcock and D. H. Boal, Biophys. J. **71**, 317 (1996); J. C. Schillcock and U. Seifert, *ibid.* **74**, 1754 (1998).
[44] P. Sens and S. A. Safran, Europhys. Lett. **43**, 95 (1998).
[45] For $A < \tilde{A}^S$ the entropic contribution to the free energy grows exponentially with δA^S (see Ref. 44) and, thus, far from $\tilde{A}^S$ it may not be ignored.